

## Dual contrast in computed tomography allows earlier characterization of articular cartilage over single contrast

Bhattacharai, Abhisek; Pouran, Behdad; Mäkelä, Janne T.A.; Shaikh, Rubina; Honkanen, Miitu K.M.; Prakash, Mithilesh; Kröger, Heikki; Grinstaff, Mark W.; Weinans, Harrie; Jurvelin, Jukka S.

**DOI**

[10.1002/jor.24774](https://doi.org/10.1002/jor.24774)

**Publication date**

2020

**Document Version**

Final published version

**Published in**

Journal of Orthopaedic Research

**Citation (APA)**

Bhattacharai, A., Pouran, B., Mäkelä, J. T. A., Shaikh, R., Honkanen, M. K. M., Prakash, M., Kröger, H., Grinstaff, M. W., Weinans, H., Jurvelin, J. S., & Töyräs, J. (2020). Dual contrast in computed tomography allows earlier characterization of articular cartilage over single contrast. *Journal of Orthopaedic Research*, 38(10), 2230-2238. <https://doi.org/10.1002/jor.24774>

**Important note**

To cite this publication, please use the final published version (if applicable). Please check the document version above.

**Copyright**

Other than for strictly personal use, it is not permitted to download, forward or distribute the text or part of it, without the consent of the author(s) and/or copyright holder(s), unless the work is under an open content license such as Creative Commons.

**Takedown policy**

Please contact us and provide details if you believe this document breaches copyrights. We will remove access to the work immediately and investigate your claim.

## RESEARCH ARTICLE

# Dual contrast in computed tomography allows earlier characterization of articular cartilage over single contrast

Abhisek Bhattarai<sup>1,2</sup>  | Behdad Pouran<sup>3</sup>  | Janne T. A. Mäkelä<sup>1</sup>  |  
Rubina Shaikh<sup>1</sup>  | Miitu K. M. Honkanen<sup>1,2</sup>  | Mithilesh Prakash<sup>1,2</sup>  |  
Heikki Kröger<sup>4</sup>  | Mark W. Grinstaff<sup>5</sup>  | Harrie Weinans<sup>3,6,7</sup> | Jukka S. Jurvelin<sup>1</sup>  |  
Juha Töyräs<sup>1,2,8</sup> 

<sup>1</sup>Department of Applied Physics, University of Eastern Finland, Kuopio, Finland

<sup>2</sup>Diagnostic Imaging Center, Kuopio University Hospital, Kuopio, Finland

<sup>3</sup>Department of Orthopaedic, University Medical Center Utrecht, Utrecht, The Netherlands

<sup>4</sup>Department of Orthopedics, Traumatology and Hand Surgery, Kuopio University Hospital, Kuopio, Finland

<sup>5</sup>Departments of Biomedical Engineering, Chemistry, and Medicine, Boston University, Boston, Massachusetts

<sup>6</sup>Department of Biomechanical Engineering, Faculty of Mechanical, Maritime, and Materials Engineering, Delft University of Technology (TU Delft), Delft, The Netherlands

<sup>7</sup>Department of Rheumatology, University Medical Center, Utrecht, The Netherlands

<sup>8</sup>School of Information Technology and Electrical Engineering, The University of Queensland, Brisbane, Australia

## Correspondence

Abhisek Bhattarai, MSc (Tech.), Department of Applied Physics, University of Eastern Finland, Finland, PO Box 1627, 70211 Kuopio, Finland. Email: [abhisek.bhattarai@uef.fi](mailto:abhisek.bhattarai@uef.fi)

## Funding information

Academy of Finland, Grant/Award Numbers: 269315, 307932; State Research Funding of the Kuopio University Hospital Catchment Area, Grant/Award Numbers: 5041746, 5041757, 5041769; Päivikki ja Sakari Sohlbergin Säätiö

## Abstract

Cationic computed tomography contrast agents are more sensitive for detecting cartilage degeneration than anionic or non-ionic agents. However, osteoarthritis-related loss of proteoglycans and increase in water content contrarily affect the diffusion of cationic contrast agents, limiting their sensitivity. The quantitative dual-energy computed tomography technique allows the simultaneous determination of the partitions of iodine-based cationic (CA4+) and gadolinium-based non-ionic (gadoteridol) agents in cartilage at diffusion equilibrium. Normalizing the cationic agent partition at diffusion equilibrium with that of the non-ionic agent improves diagnostic sensitivity. We hypothesize that this sensitivity improvement is also prominent during early diffusion time points and that the technique is applicable during contrast agent diffusion. To investigate the validity of this hypothesis, osteochondral plugs ( $d = 8$  mm,  $N = 33$ ), extracted from human cadaver ( $n = 4$ ) knee joints, were immersed in a contrast agent bath (a mixture of CA4+ and gadoteridol) and imaged using the technique at multiple time points until diffusion equilibrium. Biomechanical testing and histological analysis were conducted for reference. Quantitative dual-energy computed tomography technique enabled earlier determination of cartilage proteoglycan content over single contrast. The correlation coefficient between human articular cartilage proteoglycan content and CA4+ partition increased with the contrast agent diffusion time. Gadoteridol normalized CA4+ partition correlated significantly ( $P < .05$ ) with Mankin score at all time points and with proteoglycan content after 4 hours. The technique is applicable during diffusion, and normalization with gadoteridol partition improves the sensitivity of the CA4+ contrast agent.

## KEYWORDS

biomechanics, cartilage, cationic contrast agent, contrast-enhanced computed tomography, dual-energy CT

This is an open access article under the terms of the Creative Commons Attribution License, which permits use, distribution and reproduction in any medium, provided the original work is properly cited.

© 2020 The Authors. *Journal of Orthopaedic Research* ® published by Wiley Periodicals LLC on behalf of Orthopaedic Research Society

## 1 | INTRODUCTION

As a consequence of instantaneous impact (eg, related to sports accident), articular cartilage can become injured, leading to the development of post-traumatic osteoarthritis (PTOA).<sup>1</sup> Erosion of articular cartilage, bone remodeling, and joint inflammation are the major characteristic features of osteoarthritis (OA).<sup>2</sup> Often, only in advanced stages of the disease patients experience symptoms, such as pain and limited mobility. Therefore, PTOA is often diagnosed after irreversible damage to the cartilage has already occurred, limiting any possibility of early intervention. Early detection of cartilage damage could enable pharmaceutical or surgical interventions for preventing the progression of OA.<sup>3,4</sup> Early OA is characterized by loss of proteoglycans (PGs), leading to decreased cartilage fixed charge density, lower swelling pressure, and subsequently reduced matrix stiffness.<sup>5</sup> Fibrillation, due to collagen network disruption, also leads to decreased stiffness and increased tissue deformation under physiological loading predisposing the tissue to further degeneration.<sup>6</sup>

Today's medical imaging modalities provide multiple methods on how to quantify OA. However, they all suffer from limitations. Ultrasonography provides real-time image acquisition cost-effectively. However, the challenge in achieving perpendicularity between the ultrasound beam angle and the naturally curving cartilage surface limits accurate diagnosis.<sup>7</sup> Magnetic resonance imaging (MRI) is great for soft tissues (eg, cartilage), but it suffers from relatively long scan times and high costs.<sup>8</sup> Computed tomography (CT) imaging is substantially more accessible and affordable, and the image acquisition is swift, and the resolution superior to MRI. Further, significant advancement has been achieved with dose optimization techniques and imaging strategies in CT to reduce the radiation doses involved.<sup>9,10</sup> However, poor soft-tissue contrast prevents separating native cartilage tissue from the surrounding synovial fluid, and, thus, requires the use of contrast agents.<sup>11,12</sup>

Delayed contrast-enhanced CT (CECT) has been applied for imaging human articular cartilage *in vivo* to assess tissue morphology and composition.<sup>13</sup> The diagnosis is based on the evaluation of an anionic contrast agent distribution within cartilage after intra-articular administration. Recently, a cationic CT agent was introduced.<sup>14-16</sup> Cartilage fixed negative charge, created by PGs, provides strong electrostatic attraction to cationic agents. These distribute inside the cartilage in direct relation to the cartilage PG content.<sup>17</sup> For this reason, cationic agents offer a more sensitive technique for diagnosing the distribution of PGs in cartilage compared with conventional anionic agents.<sup>15,18-20</sup> Higher uptake of the cationic agents in cartilage provides higher X-ray attenuation and improves contrast allowing better visualization of PG distribution and its variation within cartilage. Thus, the detection of subtle changes in PG content is possible at different stages of cartilage degeneration.<sup>16,17</sup> Contrast agents diffusion in early time points is fast, especially in degenerated cartilage, due to increased permeability. The uptake of a cationic agent depends both on the electrostatic attraction between the positively charged molecule and the negative fixed charge in cartilage, and the passive diffusion controlled by cartilage water content and permeability.<sup>21</sup> Thus, in degenerated cartilage, the uptake of the cationic agent is simultaneously reduced due to the decrease of

negatively charged PGs, and enhanced due to the increase in permeability and water content. These opposite effects limit the diagnostic effectiveness of the cationic agents, especially in the first hours of diffusion, which is vital for the clinical feasibility of the agent. After intra-articular administration, contrast agents diffuse into cartilage, while simultaneously, the body clears out the agent from the joint cavity, lowering the concentration as time progresses. The concentration of anionic ioxaglate in joint cavity has been reported to be adequate for delayed-CECT until 2 hours after the administration, while the agent concentration in patellar and femoral cartilage reached the maximum 30 and 60 minutes after the administration, respectively.<sup>13</sup> The molar concentration of cationic and non-ionic agents in cartilage increases faster compared with an anionic agent.<sup>19,22</sup> Thus, considering the diffusion in cartilage and the clearing out of the contrast agents from the joint cavity, the 30 to 60 minutes imaging time window could be clinically feasible for the application of both cationic and non-ionic agents.

Contrast agent partition in cartilage is quantified as a ratio of contrast agent-induced X-ray attenuation in the cartilage relative to the attenuation in the bath.<sup>23</sup> Normalization (division) of an iodine-based cationic agent (CA4+) partition with an electrically neutral gadolinium-based agent (gadoteridol) partition improved the sensitivity of CA4+ to probe cartilage PG content after 72 hours of diffusion.<sup>24,25</sup> Because water content and permeability of cartilage control the diffusion of the non-ionic gadoteridol the normalization minimizes the effect of these factors on the diffusion of the cationic agent.<sup>25,26</sup> In early diffusion time points, contrast agent diffusion flux is high.<sup>15,22</sup> Further, the agent fluxes are even higher in a degenerated cartilage due to loss of collagen network integrity and reduced PG, resulting in increased permeability.<sup>12,25</sup> Considering this, we hypothesize that the improvement in the sensitivity of the cationic agent after normalization is even more substantial in a degenerated cartilage at early time points. Here we study the diffusion of the agents at clinically relevant time points (<1 hour after contrast agent administration) and at later diffusion time points close to diffusion equilibrium. Further, we examine the validity of the hypothesis by evaluating the sensitivity of normalized CA4+ partition to reflect variation in histopathological and biomechanical properties of human articular cartilage samples. Improvement in the sensitivity of the cationic agent would enable early detection of minor injuries and lesions, allowing timely selection of treatment, thus reducing the risk for PTOA. This quantitative technique is based on the simultaneous diffusion of two contrast agents (iodine-based CA4+ and gadolinium-based gadoteridol) into cartilage. Accurate simultaneous quantification of concentrations of two contrast agents using single X-ray tube voltage is not possible, as X-ray attenuation of both agents contributes to the attenuation. Hence, as iodine and gadolinium have different x-ray attenuation properties as a function of energy imaging with two separate X-ray tube voltages allows quantitative determination of the concentration of the elements in the mix. Determining the concentration of CA4+ and gadoteridol in cartilage is possible by using the Beer-Lambert law and Bragg's additive rule for mixtures as described in literature<sup>24-26</sup> and also in the materials and methods chapter of this paper. As the contrast agents are constantly diffusing

in cartilage during a scan, CT acquisition at two different X-ray tube voltages must be nearly instantaneous for accurate determination of contrast agent tissue partition. In this study, we also quantify the error in the partition of the contrast agents arising from the ongoing diffusion in the cartilage when the imaging is performed separately with two X-ray tube voltages.

## 2 | MATERIALS AND METHODS

### 2.1 | Sample extraction and preparation

Human osteochondral plugs ( $N = 33$ ,  $d = 8$  mm) were extracted from the lateral and medial tibial plateaus and femoral condyles in left and right knee joints of human cadavers ( $n = 4$ , mean age =  $71.25 \pm 5.18$  years).<sup>27-29</sup> The Research Committee of the Northern Savo Hospital District granted a favorable opinion on collecting the human tissue (Kuopio University Hospital, Kuopio, Finland, Decision numbers: 134/2015 and 58/2013). The samples were stored frozen in phosphate-buffered saline (PBS;  $-22^\circ\text{C}$ ).

### 2.2 | Biomechanical measurements

Samples were thawed at room temperature. A custom-made, high precision material testing device (resolution:  $0.1 \mu\text{m}$ ,  $0.005 \text{ N}$ , PM500-1 A; Newport, Irvine, CA) was employed for biomechanical testing of the osteochondral plugs.<sup>30</sup> Measurement setup schematics are included in the supplementary material (Figure S6). During the test, the plugs were immersed in PBS containing inhibitors of proteolytic enzymes ( $5 \text{ mM}$  EDTA, VWR International, and  $5 \text{ mM}$  benzamidine hydrochloride hydrate [Sigma-Aldrich Inc, St. Louis, MO]). A flat-ended metallic indenter ( $d = 728 \mu\text{m}$  [ $n = 20$ ] or  $d = 667 \mu\text{m}$  [ $n = 13$ ]) was driven in perpendicular contact with the articular surface. During the experiments, the tip of the indenter was accidentally damaged, and we had to continue the experiment with a spare indenter. The new indenter tip diameter was slightly different from the damaged indenter. However, the difference in the diameter is accounted for in the determination of the moduli values along Hayes et al.,<sup>31</sup> A pre-stress of  $12.5 \text{ kPa}$  defined the contact.<sup>32</sup> Based on literature, the Poisson ratios were set to  $\nu = (0.3(\text{Tibia}), 0.2(\text{Femur}))$  for  $E_{\text{equilibrium}}$  and  $\nu = 0.5$  for  $E_{\text{instantaneous}}$ .<sup>33,34</sup> The plugs were then again frozen, cut to two halves, and stored in a freezer ( $-22^\circ\text{C}$ ). One half was thawed for contrast-enhanced microCT imaging experiment, and the other half was prepared for reference histological analyses.

### 2.3 | MicroCT imaging

The dual-energy microCT set-up was tested and validated by quantifying iodine (I) and gadolinium (Gd) contents in phantoms with known contrast agent mixtures consisting of gadoteridol ( $20$ ,  $12$ , and  $8 \text{ mgGd/mL}$ ) and CA4+ ( $0$ ,  $10$ ,  $20$ ,  $30$ ,  $40$ ,  $50$ ,  $60$ , and  $70 \text{ mgI/mL}$ ).

Calibration curves and the measurement setup are presented in the supplementary material (Figures S7, S8, and S9). The edges of the osteochondral samples were sealed using cyanoacrylate (Super glue Precision, Loctite, Düsseldorf, Germany) to allow the contrast agent diffusion only through the articulating surface. Before the immersion in contrast agent bath, the plugs were imaged with a high-resolution microCT scanner (Quantum FX, Perkin Elmer) with an isotropic voxel size of  $40 \times 40 \times 40 \mu\text{m}$  and using a  $20 \times 20 \text{ mm}$  field of view. Three samples were arranged in a sample holder and immersed in a contrast agent bath ( $15 \text{ ml}$ ) comprised of iodine-based CA4+ ( $5,5'$ -(malonylbis(azanediyl))bis( $\text{N}^1, \text{N}^3$ -bis(2-aminoethyl)-2,4,6-triiodoisophthalamide,  $q = +4$ ,  $M = 1499.88 \text{ g/mol}$ ) and gadolinium-based gadoteridol (Prohance; Bracco International B. V., Amsterdam, Netherlands,  $q = 0$ ,  $M = 559 \text{ g/mol}$ ) diluted in PBS. The expected partitions of the contrast agents in cartilage were accounted for when designing the concentration to use for the bath, to achieve a similar relative contribution to X-ray attenuation at tube voltages of  $50$  and  $90 \text{ kVp}$ .<sup>22,26,35</sup> By doing so, the optimum signal to noise ratio was achieved while limiting excessive beam hardening and photon starvation artifacts. Based on these considerations  $10 \text{ mgI/mL}$  (CA4+) and  $20 \text{ mgGd/mL}$  (gadoteridol) were selected for the immersion bath. To prevent degradation of the samples, proteolytic inhibitors,  $5 \text{ mM}$  of ethylenediaminetetraacetic acid (EDTA, VWR International, France),  $5 \text{ mM}$  of benzamidine hydrochloride hydrate (Sigma-Aldrich Inc), and penicillin-streptomycin-amphotericin (Antibiotic Antimycotic solution, stabilized; Sigma-Aldrich Inc) were added to the bath. The samples were imaged using the Quantum FX microCT scanner at the following diffusion time points:  $10$  minutes,  $30$  minutes,  $1$ ,  $2$ ,  $3$ ,  $4$ ,  $6$ ,  $10$ ,  $21$ ,  $32$ ,  $50$ ,  $72$  hours. The osmolality of the contrast agent bath was  $297 \text{ mOsm/kg}$  measured using a commercial osmometer (Advanced Model 3320 micro-osmometer; Advanced Instruments, MA). The contrast agent bath was gently stirred throughout the immersion of the samples. The stirring assembly was placed inside a refrigerator ( $4^\circ\text{C}$ ) to preserve the cartilage and prevent bacterial and fungal growth. For microCT imaging, the samples were removed from the bath, gently blotted on the edges with blotting paper, and placed inside a humidified plastic tube. Scanning was performed using two X-ray energies (tube voltages of  $90$  and  $50 \text{ kVp}$ ). Gd and I have well-separated K-absorption edges of  $50.2$  and  $33.1 \text{ keV}$ , respectively. When using a  $50 \text{ kVp}$  tube voltage, the maximum fraction of the spectrum was selected to be between the K-edges of I and Gd to maximize the ratio of X-ray absorption caused by I and Gd ( $\mu_{\text{I}}/\mu_{\text{Gd}}$ ). Similarly, when using  $90 \text{ kVp}$ , the maximum fraction of the spectrum was selected to be above  $50 \text{ kVp}$  to maximize the  $\mu_{\text{Gd}}/\mu_{\text{I}}$  ratio (Figure S10). The tube current ( $0.2 \text{ mA}$ ) was set to the maximum value allowed by the manufacturer to improve the signal to noise ratio. Immediately after imaging, the samples were placed back into the contrast agent bath. The image acquisition time with each tube voltage was approximately  $2$  minute. Due to a human error, three samples were imaged twice using the same tube voltage at  $1$  hour diffusion time point. Thus, the partition results for those samples could not be calculated, and the  $1$  hour time point results of those samples have been excluded.

## 2.4 | Image analysis

The concentrations of iodine ( $C_I$ ) and gadolinium-based ( $C_{Gd}$ ) contrast agents in cartilage were resolved based on Beer-Lambert law and Bragg's additive rule of mixtures:

$$\alpha_E = \mu_{I(E)} C_I + \mu_{Gd(E)} C_{Gd}, \quad (1)$$

where  $\alpha$  is X-ray attenuation in a medium at energy  $E$  (tube voltages of 90 and 50 kVp) as,

$$C_I = \frac{\alpha_{(90kV)} \mu_{Gd(50kV)} - \alpha_{(50kV)} \mu_{Gd(90kV)}}{\mu_{I(90kV)} \mu_{Gd(50kV)} - \mu_{I(50kV)} \mu_{Gd(90kV)}} \quad (2)$$

$$C_{Gd} = \frac{\alpha_{(90kV)} \mu_{I(50kV)} - \alpha_{(50kV)} \mu_{I(90kV)}}{\mu_{Gd(90kV)} \mu_{I(50kV)} - \mu_{Gd(50kV)} \mu_{I(90kV)}}. \quad (3)$$

The mass attenuation coefficients for CA4+ ( $\mu_{I,E}$ ) and gadoteridol ( $\mu_{Gd,E}$ ) were determined at both energies by imaging series of contrast agent solutions with known I and Gd concentrations in distilled water, respectively. Segmentation of the articulating surface and bone-cartilage interface was done using Seg3D software (vs. 2.4.0; The University of Utah, Salt Lake City, UT). The volume of interest was defined to be  $2800 \times 2000 \mu\text{m} \times$  cartilage thickness. The X-ray attenuation profiles from the surface to deep cartilage were extracted using Matlab (R2016b; The Mathworks Inc, Natick, MA). To avoid partial volume effect arising from background and irregular and undulating surface, and cartilage-bone interface, 3% and 5% of cartilage thickness from the articular surface and cartilage-bone interface, respectively, was excluded from the attenuation profiles. X-ray attenuation profiles of the cartilage before immersion in contrast agent bath were subtracted from the contrast-enhanced cartilage profiles to obtain depth-wise attenuation profiles induced only by the contrast agents. Concentration profiles of I and Gd from the surface to the deep cartilage were calculated using Equations 2 and 3, respectively.

## 2.5 | Histological analysis and Mankin scoring

The osteochondral samples were decalcified in EDTA. Following dehydration, the EDTA decalcified samples were embedded in paraffin to be cut into  $3 \mu\text{m}$  thick sections from the center of the plug along the coronal plane (from articulating surface to the cartilage-bone interface). After removing the paraffin, the cut sections were stained with Safranin-O.<sup>36</sup> Optical density (OD) of the staining in each section was determined by applying quantitative digital densitometry technique using a light microscope (Nikon Microphot-FXA, Nikon Co, Japan) equipped with a 12-bit CCD camera (ORCA-ER; Hamamatsu Photonics K.K., Japan). For each cartilage sample, three histological sections were measured. The depth-wise OD profiles of the sections were then normalized to the length of 100 points and averaged. Before the measurements, the system was calibrated

using neutral density filters (Advanced Optics SCHOTT AG, Mainz, Germany) with OD range between 0 (low) and 3 (high).

Four independent observers (M. Honkanen, R. Shaikh, N. Hänninen, M. Prakash) assessed and assigned histopathological Mankin scoring based on the severity of OA using the Safranin-O stained sections.<sup>37</sup> Mankin score characterizes cartilage based on staining (0-4), tidemark integrity (0-1), abnormality in structure (0-6), and cellularity (0-3). Intact cartilage is assigned score 0, and a severely degenerated sample is scored 14. Mankin scores were calculated by averaging the scores of three sections per sample.

## 2.6 | Error simulation

Error in contrast agent concentrations arising from the progressing diffusion during the time between image acquisitions with two X-ray tube voltages (90 and 50 kVp) was studied using a numerical simulation. To describe the contrast agents diffusion in cartilage, equation  $C = C_{\text{max}} \times [1 - \exp(-t/\tau)]$  was fitted to the experimental data (all the samples in the present study), where  $C$  represents I and Gd concentrations in mgI/ml and mgGd/ml, respectively,  $t$  is the diffusion time (minutes) and  $\tau$  is the time required to reach 63.2% of the maximum concentration ( $C_{\text{max}}$ ).<sup>15</sup> The error simulation was implemented in steps, as follows:

Step 1. Fitting was done for each sample individually, after which a mean of the parameters ( $C_{\text{max}}$  vs  $\tau$ ) for both contrast agents was calculated (Figure 1).

Step 2. Using equation 1, X-ray attenuation was simulated with both tube voltages, based on the contrast agent concentrations obtained from the fit (step 1). This was done with varying time (2, 5, 10, 15, 30, 45, and 60 minutes) between acquisitions with the 90 and 50 kVp tube voltages. This was done for all the diffusion time points until diffusion equilibrium (72 hours).

Step 3. Using the simulated data gathered in step 2, concentrations of the contrast agents were calculated (Equations 2 and 3).

Step 4. The simulated concentration values were then compared with the true concentration values (from the fit) to get the relative error, as illustrated in Figure 5.

## 2.7 | Statistical analysis

The statistical analyses were conducted using SPSS (v. 23.0 SPSS Inc; IBM Company, Armonk, NY) statistical software. The reliability in the Mankin scoring between the raters was evaluated by determining the Interclass Correlation coefficient. Shapiro-Wilk test showed the sample data to follow the normal distribution. Therefore, the correlations of contrast agent partitions with histopathological and biomechanical reference parameters were evaluated using a parametric test (Pearson's correlation analysis) within a selected cartilage region. For all statistical tests,  $P < .05$  was set as the limit of statistical significance.

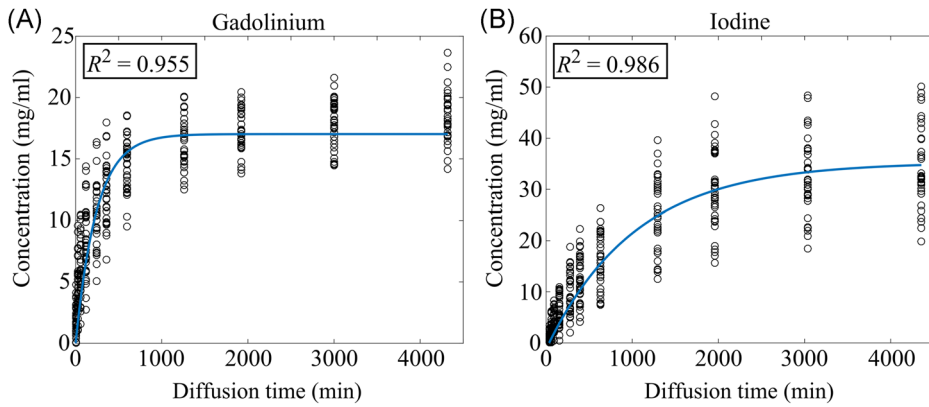


**FIGURE 1** Full thickness cartilage concentration of (A) gadoteridol (gadolinium) and (B) CA4+ (iodine) presented as a function of diffusion time,  $C_{Gd} = 17 \text{ mg/mL}$  ( $1 - \exp(-t/244 \text{ minute})$ ) and  $C_I = 35 \text{ mg/mL}$  ( $1 - \exp(-t/1032 \text{ minute})$ ), respectively [Color figure can be viewed at [wileyonlinelibrary.com](http://wileyonlinelibrary.com)]

**3 | RESULTS**

The CA4+ and gadoteridol partitions in cartilage increased from  $14.4\% \pm 8.8\%$  and  $10.2\% \pm 5.6\%$  at 10 minutes to  $344.0\% \pm 77.9\%$  and  $91.4\% \pm 9.7\%$  at 72 hours, respectively (Figures 1 and S11). The average  $C_{max}$  was 35 and 17 mg/mL, and  $\tau$  was 1032 and 244 minutes, for the iodine (CA4+) and gadolinium (gadoteridol) in the cartilage, respectively. At 72 hours, the uptake of CA4+ was 2.5 times greater in deep cartilage compared with the superficial cartilage (Figure 2). The correlation coefficients between the Mankin score and CA+ partition of the full-thickness cartilage increased at all the diffusion time points after normalizing with the partition of the non-ionic gadoteridol (Figure 3). The Mankin score correlated significantly with gadoteridol partition from 10 minutes to 10 hours after the start of the immersion in contrast agent mix. The mean OD and thickness values of the

cartilage samples were  $1.07 \pm 0.26 \text{ AU}$  (min, 0.43; max, 1.47 AU), and  $2.42 \pm 0.68 \text{ mm}$  (min, 1.01; max, 4.35 mm), respectively (Figure S12). The correlation coefficient between OD and CA4+ partition increased with the contrast agent diffusion time (Figure 4A). The correlation was significant in the earliest time points for the superficial 10% of cartilage ( $P < .029$ ). The equilibrium modulus correlated significantly with the normalized CA4+ partition after 21 hours of diffusion ( $P < .014$ ) and CA4+ partition after 32 hours of diffusion ( $P < .004$ ) (Table 1). Based on the error simulation, a 2-minute delay between the acquisitions at the 10-minute diffusion time point would result in 74.4% and 23.5% relative error in determined CA4+ and gadoteridol partitions (Figure 5). At the 100-minute time point, the errors were 6.2% and 2.2% for CA4+ and gadoteridol, respectively. The mean Mankin score of all the samples was  $6.27 \pm 1.27$  (min, 2; max, 9). The mean equilibrium modulus value for the samples was  $0.26 \pm 0.32 \text{ MPa}$  (min, 0.01;

-- 72 hour ◊ 50 hour \* 32 hour ▲ 21 hour ◆ 10 hour ◊ 6 hour ● 4 hour ▽ 2 hour ☆ 1 hour + 30 min ○ 10 min

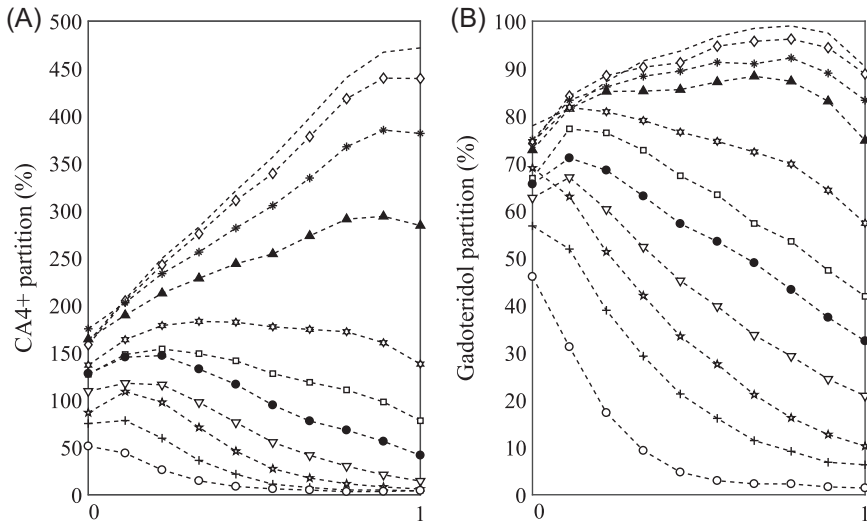


**FIGURE 2** Mean contrast agent partition profiles in cartilage ( $N = 33$ , at 1 hour time point  $N = 30$ ) in different diffusion time points; (A) Cationic iodine-based (CA4+) and (B) non-ionic gadolinium-based (gadoteridol) contrast agents. Cartilage (mean  $\pm$  SD thickness  $2.42 \pm 0.68 \text{ mm}$ ) surface is denoted with 0 and cartilage-bone interface with 1

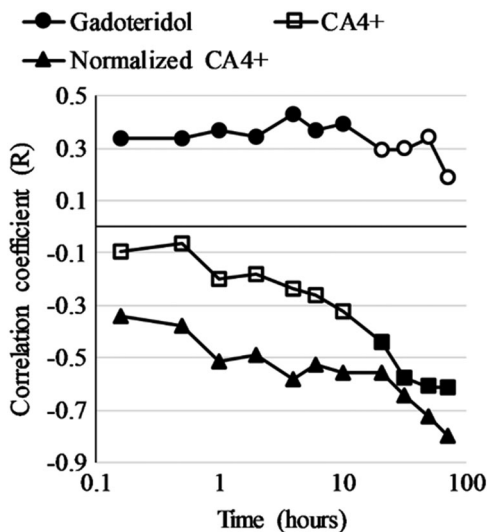


**FIGURE 3** Correlation (Pearson's) coefficient between Mankin score and gadoteridol partition, CA4+ partition and CA4+ partition normalized with gadoteridol partition in the full thickness cartilage. Filled markers indicate statistically significant ( $P < .05$ ) correlation

max, 1.49 MPa). The inter-rater reliability in the Mankin score was high (Inter-observer correlation = 0.93,  $P < .01$ ). The Kruskal-Wallis test revealed no difference ( $P > .79$ ) in the equilibrium modulus values  $0.27 \pm 0.36$  and  $0.25 \pm 0.25$  between the samples measured with indenters having tip diameters of 667 and 728  $\mu\text{m}$ , respectively.

#### 4 | DISCUSSION

In this *ex vivo* study, simultaneous diffusion of two contrast agents (CA4+ and gadoteridol) into cartilage was evaluated using a microCT scanner at multiple time points to probe cartilage composition and structural integrity. Normalization of the CA4+ partition with that of the gadoteridol improved the correlation with the Mankin score at all time points (Figure 3). Assessing cartilage structural integrity using only cationic agents at early time points is challenging as the uptake is comparably high in both intact and degenerated cartilage, due to high PG content, and increased permeability, respectively. This limits the sensitivity of cationic agents to quantify reduced PG content especially during the early points of contrast agent diffusion. Normalizing the CA4+ partition with that of gadoteridol improves its sensitivity to detect PG content. In this study, a similar effect is seen between CA4+ and PG content where the normalization with gadoteridol partition reveals a significant correlation six hours earlier, beginning at the 4-hour diffusion time point (Figure 4B).

During very early diffusion (<1 hour time points), the CA4+ significantly correlates with PG content (ie, OD,  $P < .05$ ) in the superficial zone (10% of the cartilage thickness) (Figure 4A). Upon inspecting the first 20% of cartilage thickness, the correlation starts to be significant only after 6 hours of diffusion. In this zone, the normalization does not improve correlation with PG content

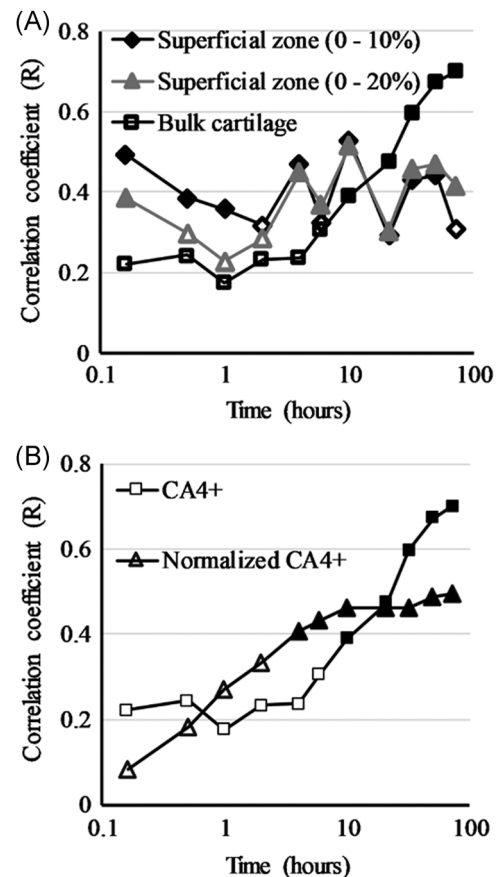


**FIGURE 4** (A) The Pearson correlation coefficient between CA4+ partition and proteoglycan content (optical density) in the superficial (10% and 20%), and full thickness cartilage as a function of diffusion time. (B) Pearson correlation coefficient between the optical density and CA4+ partition (gadoteridol partition normalized and non-normalized) as a function of diffusion time. Filled markers indicate statistically significant ( $P < .05$ ) correlation

(Table S1). This is likely due to the partial volume effect. In the full thickness cartilage, the correlation with PG content is relatively weak at early time points. However, with the diffusion of CA4+ into deep cartilage, the correlation becomes stronger and is significant ( $P < .05$ ) after 10 hours of diffusion. The partition of CA4+ increases towards the deep cartilage at later diffusion time points (Figure 2). This is due to the increased electrostatic attraction, resulting from high PG content in the deep cartilage (Figure S13).<sup>38,39</sup> Concurrently, the water content in cartilage decreases towards the cartilage-bone interface.<sup>5</sup> Thus, expecting the gadoteridol partition to follow the trend of water content in cartilage, it is surprising to see the higher partitions in the deeper zones after the 21-hour diffusion time point. We suspect that this is a result of X-ray beam hardening, as very high uptake of the cationic agent is observed post 21-hour imaging time-point in the PG rich deep cartilage (Figure 2). Based on the present experiments and the results, we cannot determine whether the high CA4+ flux could have caused drag influencing the gadoteridol diffusion.<sup>40</sup> Additionally, the overall gadoteridol partition is not observed to rise after a 10-hour imaging time-point (Figure 1A).

**TABLE 1** Pearson's correlation coefficients between contrast agent partitions ( $N = 33$ , at 1 h time point  $N = 30$ ) and biomechanical moduli

	Time, min		Time, h								
	10	30	1	2	4	6	10	21	32	50	72
Equilibrium modulus, MPa											
CA4+	0.008	-0.129	0.156	0.071	0.162	0.186	0.209	0.311	<b>0.493**</b>	<b>0.521**</b>	<b>0.497**</b>
Normalized CA4+	0.212	-0.139	0.122	0.032	0.260	<b>0.330*</b>	0.293	<b>0.422*</b>	<b>0.654**</b>	<b>0.730**</b>	<b>0.648**</b>
Gadoteridol	-0.218	-0.105	-0.192	-0.126	-0.246	-0.285	-0.246	-0.339	<b>-0.471*</b>	<b>-0.453*</b>	-0.282
Instantaneous modulus, MPa											
CA4+	-0.120	-0.048	0.223	0.131	0.172	0.182	0.131	0.169	0.216	0.209	0.176
Normalized CA4+	<b>0.534**</b>	-0.064	0.177	0.043	0.170	0.248	0.178	0.213	<b>0.359*</b>	<b>0.339*</b>	<b>0.290*</b>
Gadoteridol	-0.281	0.022	-0.124	0.035	-0.085	-0.140	-0.147	-0.176	<b>-0.441**</b>	<b>-0.344*</b>	-0.272

\*Indicates that correlation is significant at the level  $P < .05$  (two-tailed).

\*\*Bold value Indicates that correlation is significant at the level  $P < .01$  (two-tailed).

The correlation between the equilibrium modulus and CA4+ partition was significant and strengthened by the normalization after 21 hours until diffusion equilibrium. This was expected as the cationic agent's uptake is mostly due to the attraction to PG's, which controls cartilage biomechanical equilibrium response.<sup>41</sup> Therefore, it is natural that the CA4+ which is attracted by the PGs correlates strongly with equilibrium modulus.

Previously, we applied the QDECT technique to evaluate the cartilage PG and water contents at diffusion equilibrium (ie, after 72 hours of diffusion).<sup>24,25</sup> In the current study, we demonstrate the simultaneous determination of the solute concentration of two contrast agents in cartilage during diffusion at clinically relevant time points. The precise determination of the contrast agent partitions at early time points is possible with the use of short scan times (Figure 5).<sup>15,24</sup> In our previous study, reliable measurements during diffusion were impossible due to long imaging acquisition time (total of 28 minutes with two tube voltages) required by the applied microCT scanner (Skyscan 1172, Skyscan, Kontich, Belgium).<sup>24</sup> With dual-contrast method, if the imaging is performed separately, an unavoidable error arises in the determination of partition of the contrast agent in cartilage. This is due to the ongoing

diffusion during the imaging (in this study the time difference between acquisitions being ~2 minutes). In the present study, we evaluate this error using numerical simulations. An increase in time difference between the CT scans results in a higher error in the determined contrast agent partition values (Figure 5). The relative error is higher for CA4+ due to the higher diffusion flux of the cationic agent compared with that of the non-ionic gadoteridol. The short scan time enabled attenuation measurements of multiple contrast agents during diffusion, and more importantly, in the clinically relevant time points. With a modern dual-energy full-body CT scanner, the image acquisition at separate energies is simultaneous and practically instantaneous.<sup>26</sup> Hence, for the clinical application of the QDECT, this is not a source of significant error. However, the simulations will aid in the planning of the QDECT studies when imaging at two energies is performed separately.

The authors acknowledge limitations related to this study. The osteochondral plugs were extracted from a limited number of cadavers and from various locations: femur (lateral condyle = 4, medial condyle = 10), tibia (lateral plateau = 8, medial plateau = 7), and trochlea = 4. The availability of the cadaveric samples determined the sample size. As this was an exploratory study, and the effectiveness of the dual-contrast

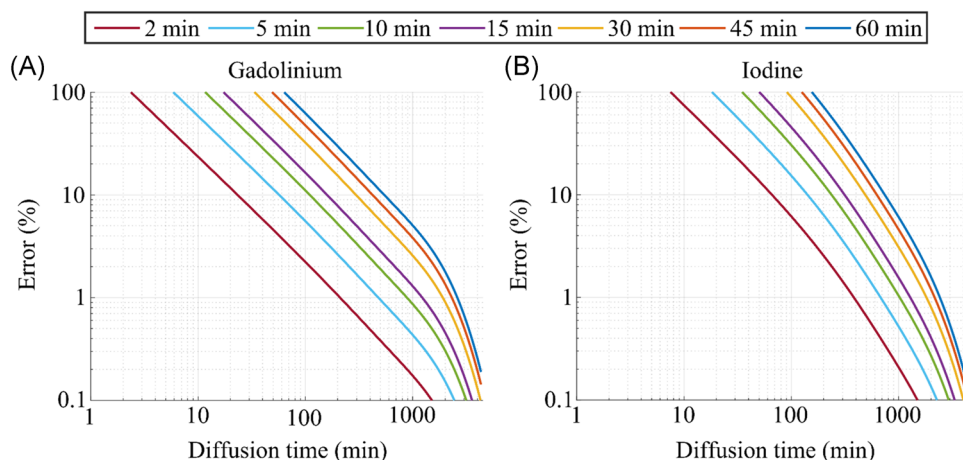


**FIGURE 5** Simulation of error in (A) gadoteridol and (B) CA4+ partitions resulting from time (2 to 60 minutes) between acquisitions with the two X-ray tube voltages (90 and 50 kVp) [Color figure can be viewed at [wileyonlinelibrary.com](http://wileyonlinelibrary.com)]

technique over the use of a single contrast agent in cartilage diagnostics was unknown, a power analysis was not conducted. Author's acknowledge that a higher number of samples would have enabled a more reliable evaluation of the diagnostic potential of the technique. The contrast agents' concentrations were selected to achieve the highest signal to noise ratio with the microCT scanner and toxicity issues were not taken into consideration. The development and introduction of a commercial clinical dual contrast application are not within the scope of this study, and the techniques may in the future rely on formulations differing from the ones applied here. The authors acknowledge the possibility of changes in cartilage properties arising from freeze-thaw cycles.<sup>42</sup> However, as all the samples were frozen and thawed following a uniform protocol, any changes in the mechanical/biological state between the samples should be similar.

The samples were immersed in the contrast agent bath maintained at 4°C. This temperature is lower than that during the intended clinical application of the agents in the human body (37°C). The time constant  $\tau$  of CA4+ was 1032 minutes, being much higher than the value reported for diffusion in bovine cartilage at room temperature ( $\tau=104.4$  minutes, cartilage edges not sealed) (Figure 2).<sup>15,43</sup> With an increase in temperature, the diffusion rate of the contrast agent will also increase. Hence, at a warmer temperature, contrast agent diffusion will be faster, and reliable assessment of cartilage integrity may be conducted at earlier diffusion time point.

The challenges associated with the clinical application of the QDECT are yet to be explored. In the future, the QDECT should be tested on full knee joints using a clinical CT device, to obtain quantitative information on the capability of the technique to reveal cartilage matrix water and PG contents. In this study, we have demonstrated that QDECT allows the simultaneous determination of two different contrast agents in cartilage from early diffusion time-point (10 minutes) until diffusion equilibrium (72 hours). Normalization of the cationic contrast agent (CA4+) partition with that of the electrically neutral contrast agent (gadoteridol) enhances correlations with the histopathological and biomechanical characteristics allowing swifter determination of cartilage integrity. Thus, QDECT has the potential for diagnosis of cartilage degeneration at clinically relevant imaging time points.

## ACKNOWLEDGMENTS

Antti Joukainen (MD), Tuomas Virén (PhD) and Juuso T.J. Honkanen (PhD) are acknowledged for assistance in sample extraction, and Amit N. Patwa (PhD) for preparing the CA4+ contrast agent. Sandra Sefa, (MSc) is acknowledged for assistance with the biomechanical measurements. Annina E.A. Saukko is acknowledged for assistance in sample holder preparation. Lassi Rieppo, Tarja Huhta, and Linda Rantamaa are acknowledged for the preparation of the histological section and Nina Hänninen for Mankin scoring of the cartilage sections. Academy of Finland (Projects 269315, 307932), State Research Funding of the Kuopio University Hospital Catchment Area (projects 5041746, 5041757, 5041769, PY210), and Päivikki and Sakari Sohlberg Foundation are acknowledged for financial support. Funding sources had no role in the design of the study, analysis, and interpretation of the results, or writing and submission of the manuscript for publication.

## CONFLICT OF INTERESTS

Dr. Grinstaff reports a patent pending on CA4+ composition. The other co-authors declare no conflict of interests.

## AUTHOR CONTRIBUTIONS

AB, BP, and JT designed the study. HK applied for ethical approval to obtain the cartilage samples. AB, MP, and, MH conducted the biomechanical measurements and analyses. RS, MP and, MH performed digital densitometry measurements and analyses. CA4+ was prepared in the laboratory of MG. Contrast agent diffusion measurements were conducted by AB and BP in the laboratory of HHW. AB, JM, and JT were involved in data analysis and interpretation of the results. AB drafted the manuscript and all co-authors contributed to the critical revision of the manuscript. All authors have read and approved the final version of the submitted manuscript.

## ORCID

Abhisek Bhattarai  <http://orcid.org/0000-0003-3713-1349>  
 Behdad Pouran  <https://orcid.org/0000-0003-1585-4917>  
 Janne T. A. Mäkelä  <https://orcid.org/0000-0002-6123-1262>  
 Rubina Shaikh  <https://orcid.org/0000-0003-4184-8254>  
 Miitu K. M. Honkanen  <http://orcid.org/0000-0002-2548-4457>  
 Mithilesh Prakash  <https://orcid.org/0000-0002-3853-4126>  
 Heikki Kröger  <https://orcid.org/0000-0003-4245-8186>  
 Mark W. Grinstaff  <http://orcid.org/0000-0002-5453-3668>  
 Jukka S. Jurvelin  <https://orcid.org/0000-0001-6317-6685>  
 Juha Töyräs  <https://orcid.org/0000-0002-8035-1606>

## REFERENCES

1. Ali TS, Prasadam I, Xiao Y, Momot KI. Progression of post-traumatic osteoarthritis in rat meniscectomy models: comprehensive monitoring using MRI. *Sci Rep*. 2018;8(1):6861.
2. Walker JA. Osteoarthritis: pathogenesis, clinical features, and management. *Nurs Stand*. 2009;24(1):35-40.
3. Olson SA, Furman BD, Kraus VB, Huebner JL, Guilak F. Therapeutic opportunities to prevent post-traumatic arthritis: lessons from the natural history of arthritis after articular fracture. *J Orthop Res*. 2015;33(9):1266-1277.
4. Bay-Jensen A-C, Hoegh-Madsen S, Dam E, et al. Which elements are involved in reversible and irreversible cartilage degradation in osteoarthritis? *Rheumatol Int*. 2010;30(4):435-442.
5. Mow VC, Ratcliffe A, Poole AR. Cartilage and diarthrodial joints as paradigms for hierarchical materials and structures. *Biomaterials*. 1992;13(2):67-97.
6. Saarakkala S, Julkunen P, Kiviranta P, Makitalo J, Jurvelin JS, Korhonen RK. Depth-wise progression of osteoarthritis in human articular cartilage: investigation of composition, structure and biomechanics. *Osteoarthr Cartil*. 2010;18(1):73-81.
7. Kaleva E, Saarakkala S, Jurvelin JS, Viren T, Toyras J. Effects of ultrasound beam angle and surface roughness on the quantitative ultrasound parameters of articular cartilage. *Ultrasound Med Biol*. 2009 Aug;35(8):1344-1351.
8. Matzat SJ, Kogan F, Fong GW, Gold GE. Imaging strategies for assessing cartilage composition in osteoarthritis. *Curr Rheumatol Rep*. 2014;16(11):462. Nov.
9. Gilbert ES. Ionising radiation and cancer risks: what have we learned from epidemiology? *Int J Radiat Biol [Internet]*. 2009;85(6):467-482. <https://www.ncbi.nlm.nih.gov/pubmed/19401906>

10. Jang J, Jung SE, Jeong WK, et al. Radiation doses of various CT protocols: a multicenter longitudinal observation study. *J Korean Med Sci.* 2016;31(suppl 1):S24-S31.
11. Kallioniemi AS, Jurvelin JS, Nieminen MT, Lammi MJ, Töyräs J. Contrast agent enhanced pQCT of articular cartilage. *Phys Med Biol.* 2007; 52(4):1209-1219.
12. Kokkonen HT, Jurvelin JS, Tiitu V, Töyräs J. Detection of mechanical injury of articular cartilage using contrast enhanced computed tomography. *Osteoarthr Cartil.* 2011;19(3):295-301.
13. Kokkonen HT, Aula AS, Kröger H, et al. Delayed computed tomography arthrography of human knee cartilage in vivo. *Cartilage.* 2012; 3(4):334-341.
14. Joshi NS, Bansal PN, Stewart RC, Snyder BD, Grinstaff MW. Effect of contrast agent charge on visualization of articular cartilage using computed tomography: exploiting electrostatic interactions for improved sensitivity. *J Am Chem Soc.* 2009;131(37):13234-13235.
15. Stewart RC, Bansal PN, Entezari V, et al. Contrast-enhanced CT with a high-affinity cationic contrast agent for imaging ex vivo bovine, intact ex vivo rabbit, and in vivo rabbit cartilage. *Radiology.* 2013;266(1):141-150.
16. Bansal PN, Joshi NS, Entezari V, et al. Cationic contrast agents improve quantification of glycosaminoglycan (GAG) content by contrast enhanced CT imaging of cartilage. *J Orthop Res.* 2011;29(5):704-709.
17. Lakin BA, Snyder BD, Grinstaff MW. Assessing cartilage biomechanical properties: techniques for evaluating the functional performance of cartilage in health and disease. *Annu Rev Biomed Eng.* 2017;19:27-55.
18. Bansal PN, Stewart RC, Entezari V, Snyder BD, Grinstaff MW. Contrast agent electrostatic attraction rather than repulsion to glycosaminoglycans affords a greater contrast uptake ratio and improved quantitative CT imaging in cartilage. *Osteoarthr Cartil.* 2011;19(8):970-976.
19. Lakin BA, Ellis DJ, Shelofsky JS, Freedman JD, Grinstaff MW, Snyder BD. Contrast-enhanced CT facilitates rapid, non-destructive assessment of cartilage and bone properties of the human metacarpal. *Osteoarthr Cartil.* 2015;23(12):2158-2166.
20. Weatherley ND, Eaden JA, Stewart NJ, et al. Contrast-enhanced computed tomography scoring system for distinguishing early osteoarthritis disease states: a feasibility study. *J Orthop Res.* 2019;74:611-619.
21. Adair GS. On the Donnan equilibrium and the equations of Gibbs. *Science.* 1923;58(1488):13.
22. Silvast TS, Kokkonen HT, Jurvelin JS, Quinn TM, Nieminen MT, Töyräs J. Diffusion and near-equilibrium distribution of MRI and CT contrast agents in articular cartilage. *Phys Med Biol [Internet].* 2009; 54(22):6823-6836. <http://www.ncbi.nlm.nih.gov/pubmed/19864699>
23. Silvast TS, Jurvelin JS, Tiitu V, Quinn TM, Toyras J. Bath concentration of anionic contrast agents does not affect their diffusion and distribution in articular cartilage in vitro. *Cartilage.* 2013;4(1):42-51.
24. Bhattarai A, Honkanen JTJ, Myller KAH, et al. Quantitative dual contrast CT technique for evaluation of articular cartilage properties. *Ann Biomed Eng.* 2018;46(7):1038-1046.
25. Saukko AEA, Turunen MJ, Honkanen MKM, et al. Simultaneous quantitation of cationic and non-ionic contrast agents in articular cartilage using synchrotron microCT imaging. *Sci Rep.* 2019;9(1):7118.
26. Honkanen MKM, Matikka H, Honkanen JTJ, et al. Imaging of proteoglycan and water contents in human articular cartilage with full-body CT using dual contrast technique. *J Orthop Res.* 2019;37:1059-1070.
27. Mirahmadi F, Koolstra JH, Fazaeli S, et al. Diffusion of charged and uncharged contrast agents in equine mandibular condylar cartilage is not affected by an increased level of sugar-induced collagen cross-linking. *J Mech Behav Biomed Mater.* 2019;90:133-139.
28. Lattanzi R, Petchprapa C, Ascani D, et al. Detection of cartilage damage in femoroacetabular impingement with standardized dGEMRIC at 3 T. *Osteoarthr Cartil.* 2014;22(3):447-456.
29. Rautiainen J, Nieminen MT, Salo E-N, et al. Effect of collagen cross-linking on quantitative MRI parameters of articular cartilage. *Osteoarthr Cartil.* 2016;24(9):1656-1664.
30. Julkunen P, Korhonen RK, Herzog W, Jurvelin JS. Uncertainties in indentation testing of articular cartilage: a fibril-reinforced poroviscoelastic study. *Med Eng Phys.* 2008;30(4):506-515.
31. Hayes WC, Keer LM, Herrmann G, Mockros LF. A mathematical analysis for indentation tests of articular cartilage. *J Biomech.* 1972; 5(5):541-551. Sep.
32. Makela JTA, Han S-K, Herzog W, Korhonen RK. Very early osteoarthritis changes sensitively fluid flow properties of articular cartilage. *J Biomech.* 2015;48(12):3369-3376.
33. Fick JM, Huttu MRJ, Lammi MJ, Korhonen RK. In vitro glycation of articular cartilage alters the biomechanical response of chondrocytes in a depth-dependent manner. *Osteoarthr Cartil [Internet].* 2014;22(10):1410-1418. <http://linkinghub.elsevier.com/retrieve/pii/S1063458414011935>
34. Kiviranta P, Rieppo J, Korhonen RK, Julkunen P, Toyras J, Jurvelin JS. Collagen network primarily controls Poisson's ratio of bovine articular cartilage in compression. *J Orthop Res.* 2006;24(4):690-699.
35. Lakin BA, Grasso DJ, Stewart RC, Freedman JD, Snyder BD, Grinstaff MW. Contrast enhanced CT attenuation correlates with the GAG content of bovine meniscus. *J Orthop Res.* 2013;31(11):1765-1771.
36. Kiviranta I, Jurvelin J, Tammi M, Saamanen AM, Helminen HJ. Microspectrophotometric quantitation of glycosaminoglycans in articular cartilage sections stained with Safranin O. *Histochemistry.* 1985; 82(3):249-255.
37. Mankin HJ, Dorfman H, Lippiello L, Zarins A. Biochemical and metabolic abnormalities in articular cartilage from osteoarthritic human hips. II. Correlation of morphology with biochemical and metabolic data. *J Bone Joint Surg Am.* 1971;53(3):523-537.
38. Buschmann MD, Grodzinsky AJ. A molecular model of proteoglycan-associated electrostatic forces in cartilage mechanics. *J Biomech Eng.* 1995;117(2):179-192.
39. Bashir A, Gray ML, Boutin RD, Burstein D. Glycosaminoglycan in articular cartilage: in vivo assessment with delayed Gd(DTPA)(2)-enhanced MR imaging. *Radiology.* 1997;205(2):551-558.
40. Honkanen MKM, Saukko AEA, Turunen MJ, et al. Synchrotron microCT reveals the potential of the dual contrast technique for quantitative assessment of human articular cartilage composition. *J Orthop Res.* 2019.
41. Canal Guterl C, Hung CT, Ateshian GA. Electrostatic and non-electrostatic contributions of proteoglycans to the compressive equilibrium modulus of bovine articular cartilage. *J Biomech.* 2010;43(7):1343-1350.
42. Peters AE, Comerford EJ, Macaulay S, Bates KT, Akhtar R. Micro-mechanical properties of canine femoral articular cartilage following multiple freeze-thaw cycles. *J Mech Behav Biomed Mater.* 2017;71: 114-121.
43. Albert Einstein. In: Furth R, On the movement of small particles suspended in a stationary liquid demanded by the molecular kinetic theory of heat. ed. *Investigations on the Theory of the, Brownian Movement.* Dover Publications, Inc; 1956.

## SUPPORTING INFORMATION

Additional supporting information may be found online in the Supporting Information section.

**How to cite this article:** Bhattarai A, Pouran B, Mäkelä JTA, et al. Dual contrast in computed tomography allows earlier characterization of articular cartilage over single contrast. *J Orthop Res.* 2020;38:2230-2238. <https://doi.org/10.1002/jor.24774>